Detection of Crustal Movement From TerraSAR-X Intensity Images for the 2011 Tohoku, Japan Earthquake

Wen Liu, *Student Member, IEEE*, and Fumio Yamazaki, *Member, IEEE*

***Abstract*—Significant crustal movements were caused by the 2011 Tohoku, Japan earthquake. A method for capturing the surface movements from pre- and postevent TerraSAR-X (TSX) intensity images is proposed in this letter. Because the shifts of unchanged buildings were considered as crustal movements in the two synthetic aperture radar images, we first extracted buildings from the pre- and postevent images using a segmentation approach. Then, the unchanged buildings were detected by matching the buildings in the pre- and postevent images at similar locations. Finally, the shifts were calculated by area-based matching. The method was tested on the TSX images covering the Sendai area. Compared with GPS observation records, the proposed method was found to be able to detect crustal movement at a subpixel level.**

***Index Terms*—Correlation, earthquakes, geophysical measurement, radar remote sensing.**

I. Introduction

THE M_w 9.0 Tohoku earthquake, which occurred on March 11, 2011, off the Pacific coast of northeastern (Tohoku) Japan, caused gigantic tsunamis, resulting in widespread devastation. The epicenter was located at 38.322° N, 142.369° E at a depth of about 32 km. The earthquake resulted from a thrust fault on the subduction zone plate boundary between the Pacific and North American plates. According to the GPS Earth Observation Network System, Geospatial Information Authority (GSI), Japan, crustal movements with maximums of 5.3 m in the horizontal (southeast) and 1.2 m in the vertical (downward) directions were observed over a wide area [1]. Although GSI has established about 1200 GPS ground control stations throughout Japan, the distance between two neighboring stations is over 20 km. Hence, it remains difficult to capture a detailed crustal movement distribution using only GPS recording data. Also, developing countries are unable to establish GPS recording systems. Thus, measuring crustal movements estimated from satellite data constitutes an efficient and important method.

Two methods have normally been used to detect crustal movements in remote sensing images in the past studies. The first is interferometric analysis of synthetic aperture radar (SAR) [2]. Several studies have been conducted to detect displacements due to earthquakes based on differential SAR interferometry [3], [4]. However, depending on vegetation and temporal decorrelation [5], interferometric SAR (InSAR) may not always be able to measure ubiquitous deformation at a large scale. The second method is the pixel-offset method, which can be applied to both SAR and optical images. Michel *et al.* [6] and Tobita *et al.* [7] measured ground displacements after earthquakes using SAR amplitude images. Crippen [8], Leprince *et al.* [9], and González *et al.* [10] also detected ground deformation in SPOT and IRS panchromatic imageries. Using the method, two images are coregistered for nondisplaced boundaries before internal local deformation is calculated by cross-correlation. Three-dimensional surface displacement estimates have been obtained by InSAR and pixel-offset methods using GPS records and SAR image pairs captured from ascending and descending orbits [11]–[13]. In the 2011 Tohoku earthquake, the extent of crustal movements was much larger than the SAR imaging area. Due to the absence of the accurate geocoding information, it was difficult to detect the absolute displacement using the previous methods. The high-accuracy georeferenced product, however, has become available recently due to the improvement of SAR sensors, and thus, we used it to estimate the absolute ground displacements even in the case of large-scale tectonic movements.

In this letter, pre- and postevent TerraSAR-X (TSX) intensity images from the Tohoku earthquake were used to detect crustal movements based on the shifts of unchanged buildings. The accuracy of the proposed method was demonstrated by comparing the detected displacements with those from GPS ground station records.

II. Image Data and Preprocessing

This study area was focused on the coastal zone of Tohoku, Japan, as shown in Fig. 1(a), which was one of the most severely affected areas during the 2011 Tohoku earthquake. Four temporal TSX images taken before and after the earthquake are shown in Fig. 1(b)–(e), which we used for detecting crustal movements. The pre-event image was taken on October 20, 2010 Universal Time, Coordinated (UTC), while the postevent ones were taken on March 12 (2 days after the earthquake) and 23 and April 3, 2011. There is a 37.31° incident angle at the center of the images. All images were captured with horizontal transmit and horizontal receive (HH) polarization and in a descending path. The images were acquired in the strip-map mode, and thus, both the azimuth resolution and

Manuscript received September 30, 2011; revised April 18, 2012; accepted April 23, 2012. This work was supported by the SAR Data Application Research Committee funding the TerraSAR-X images used in this study that were provided to the present authors by Pasco Corporation, Tokyo, Japan.

The authors are with the Department of Urban Environment Systems, Chiba University, Chiba 265-8522, Japan (e-mail: wen_liu@graduate.chiba-u.jp; yamazaki@tu.chiba-u.ac.jp).

Color versions of one or more of the figures in this paper are available online at http://ieeexplore.ieee.org.

Digital Object Identifier 10.1109/LGRS.2012.2199076

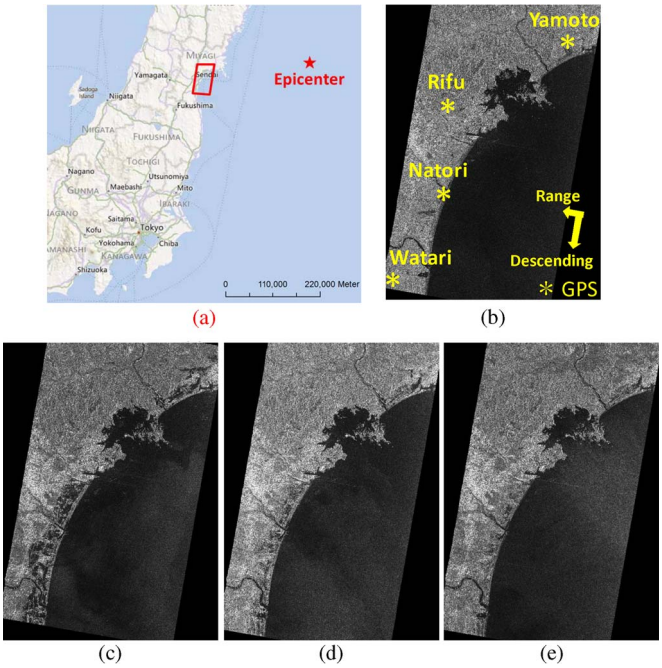

Fig. 1. (a) Study area along the Pacific coast of Tohoku, Japan, including four GPS ground stations: Pre-event TSX image taken on (b) October 21, 2010, and the postevent images taken on (c) March 13, (d) 24, and (e) April 4, 2011.

the ground-range resolution were about 3.3 m. We used the orthorectified multilook corrected products [enhanced ellipsoid corrected (EEC)] provided by Deutsches Zentrum für Luft- und Raumfahrt (DLR), where the image distortion caused by a variable terrain height was compensated for by using a globally available digital elevation model (DEM) (shuttle radar topography mission). The products were provided in the form projected to a World Geodetic System 84 reference ellipsoid with a resampled square pixel size of 1.25 m.

Two preprocessing approaches were applied to the images before extracting crustal movements. First, the four TSX images were transformed to a sigma-naught (σ^0) value, which represents the radar reflectivity per unit area in the ground range. A Lee filter was then applied to the original SAR images to reduce the speckle noise. To minimize any loss of information included in the intensity images, the window size of the filter was set as 3×3 pixels. The pixel localization corrected by the GPS orbit determination was used directly in this study. According to the product specification document [14], the pixel localization accuracy of EEC products depends on the orbit and the DEM used. Since the four EEC products were made using the same DEM following the same process, the errors caused by DEM were cancelled out when comparing two images [15]. Thus, the major cause of error here comes from orbit accuracy. Since the orbit type of our TSX images was "Science," their required orbit accuracy is within 20 cm, but actual data showed better than 10-cm accuracy [16].

III. Movement Detection Methodology

This study proposes a method for detecting crustal movements based on the measurement of the displacements of unchanged buildings in two SAR intensity images. Currently, crustal movements are often detected by registering the ground surface. However, during the Tohoku earthquake, gigantic tsunamis hit many cities/towns along the coast, and the ground surface was changed significantly by debris or flooded seawater. Thus, this study focused on the displacements of unchanged buildings to ensure stable and high correlation. First, segmentation was performed on a pair of images to extract the location of building objects. Next, matching was used to detect unchanged buildings in the two images. The displacements of the unchanged buildings were calculated using an area-based matching method. Finally, the average shift for all the unchanged buildings in an area was calculated, and it was considered as the crustal movement there.

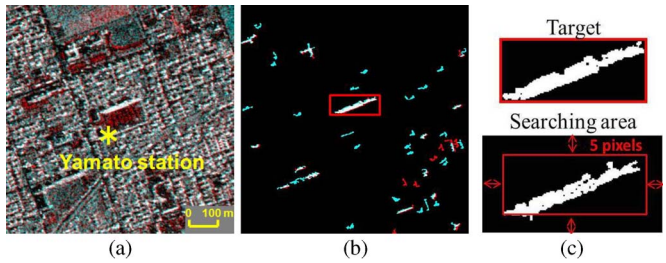

Fig. 2. (a) Color composition of pre- and postevent TSX images and (b) building images [(red) 2011/03/13, (green and blue) 2010/10/21]. (c) Target building object in the pre-event and the search area in the postevent building image.

A. Segmentation

In most cases, buildings show higher backscatter than other surface objects in SAR images because of their corner reflection. To detect the locations of buildings, we divided the pre- and postevent TSX images into the objects (pixel groups) based on the pixel digital number values. According to a visual inspection of the histograms of the SAR images, the threshold value of the backscattering coefficient between buildings and other objects was set as -2.0 dB. Based on a typical building size, only objects larger than 100 pixels were extracted as engineered (solid) buildings. Thus, objects with the average backscattering coefficient greater than -2.0 dB and with the size larger than 100 pixels were extracted, and those were used in the next step. A part of the color composition of the pre- and postevent TSX images around the Yamoto GPS station is shown in Fig. 2(a), while the building images are shown in Fig. 2(b). Obvious shifts can be seen in the shapes of the same buildings between the images.

B. Extraction of Unchanged Buildings

The tsunami caused by the earthquake affected vast amounts of coastal areas, so many constructions such as wooden houses and seawalls were destroyed or carried away. Thus, the shifts of unchanged (solid) buildings had to be observed to measure the crustal movements. A building object extracted from the pre-event building image was selected as a target object. A rectangular area surrounding the target building and exceeding its size was then selected from the postevent building image as the search area. An example of the target and search areas is shown in Fig. 2(c). If a building object existed in this area, then the target building was considered as unchanged. Based on GPS stations' data, the maximum crustal movement observed during this event was about 5 m in the horizontal and 1 m in the vertical

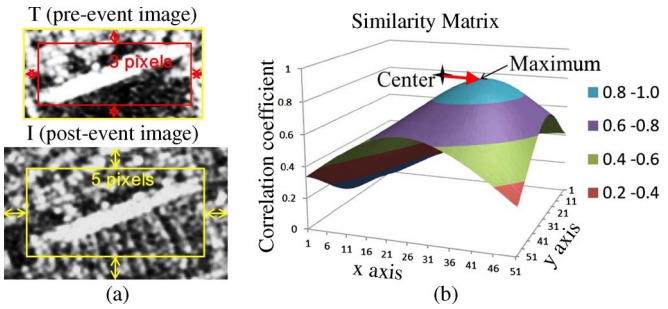

Fig. 3. (a) Target area T in the pre-event SAR image and the search area I surrounding the target area in the postevent image. (b) Similarity matrix for the target and search areas.

directions, and thus, the search area was set as five pixels (6.25 m) larger than the target object in the two horizontal directions.

C. Calculation of Displacements

After detecting the locations of unchanged buildings, the shifts of the building shapes due to the event were calculated using an area-based method. The target area (T) was selected from the pre-event intensity image in the locations of unchanged building objects, which were extracted in the previous step. To improve the accuracy of area-based matching, the ground surface surrounding a building object within a distance of three pixels was also included in the target area. The search area (I), which surrounds the target area and exceeds it in size, was selected in the postevent intensity image. Examples of T and I are shown in Fig. 3(a). The target and search areas were resampled to 0.25 m/pixel by cubic convolution to have 1/5 of the original pixel size. The shift of building shapes could then be detected at a subpixel level.

Area correlation is a method used for designating ground control points during image-to-image registration. In this letter, the target area was overlaid with the search area, and a similarity index was calculated. The similarity matrix contained the values of the statistical comparison between the target and search areas. The position in the similarity matrix where the similarity index reached a maximum value represented the necessary offset that the target had to move along the x- and y-axes to match the searching area.

An example of a calculated similarity matrix is shown in Fig. 3(b). The target and search areas were selected with the same center point, so the maximum value should be at the center of the matrix if no movement occurred. In this case, the building moved 11 pixels to the east and five pixels to the south, which indicates that the crustal movement in this area was 2.75 m to the east and 1.25 m to the south.

IV. Results

The TSX images were divided into a square mesh containing 4000 × 4000 pixels (25 km^2), to detect the ground movements. The movements of unchanged buildings were calculated in each subarea, and the average value was considered to be the crustal movement of that subarea. A square including the GPS ground control station, known as Yamoto, is shown in Fig. 4(a). We extracted 325 buildings from the pre-event image,

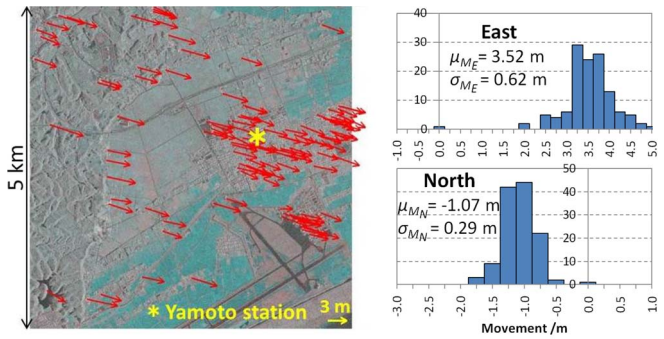

Fig. 4. (a) Results showing the displacement vectors detected between October 21, 2010, and March 13, 2011, images, which overlap on the color composite of the TSX intensity images, with a subarea including Yamoto GPS station. (b) Histograms showing the displacement in the east and north directions.

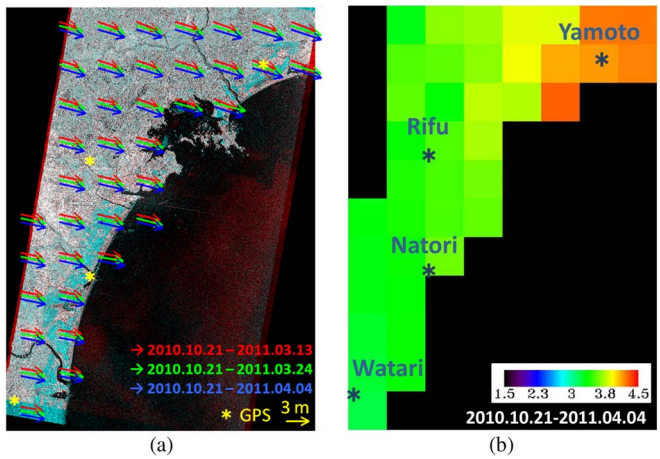

Fig. 5. (a) Detected displacement vectors in each subarea in the periods October 21, 2010–March 13, 2011, October 21, 2010–March 24, 2011, and October 21, 2010–April 4, 2011, overlapping on the color composite of the TSX intensity images and (b) displacement amplitude values from October 21, 2010, to April 4, 2011, shown in rainbow color.

whereas 207 buildings were detected as unchanged between the October 21, 2010, and March 13, 2011, images. These buildings were mostly distributed outside the areas inundated by tsunami. To ensure that the pre-event building matched with the same postevent building correctly, only the shift of a building with a similarity index higher than 0.8 was counted as a crustal movement. Using this method, the shifts of 124 buildings were detected in this square area, and their movement vectors are shown in Fig. 4(a). Histograms of the movements in the east and north directions are shown in Fig. 4(b). The mean value of the displacement was 3.72 m, heading toward 107.05° clockwise from the north.

The crustal movements over the whole area were detected in the same way. To ensure the reliability of the results, only a subarea containing more than ten building displacements was counted as a valid subarea. Fortunately, all the subareas in this study area were valid. The displacement vectors are shown in Fig. 5(a). The displacements of the four subareas including GPS stations are also shown in Table I. A comparison of the detected movements in the table shows that the largest movement occurred around Yamoto GPS station and the value was getting smaller when going southward.

TABLE I
DETECTED CRUSTAL MOVEMENTS IN FOUR SUBAREAS SURROUNDING THE GPS STATIONS OVER THREE PERIODS (UNIT: IN METERS)

Period	Method	Yamato station		Rifu station		Natori station		Watari station	
		East	North	East	North	East	North	East	North
2010/10/21 to 2011/03/13	TSX	**3.52**	-1.07	3.03	-0.72	3.01	-0.49	2.77	-0.42
	GPS data	3.24	-1.06	2.77	-0.73	2.73	-0.61	2.45	-0.42
2011/03/13 to 2011/03/24	TSX	0.31	-0.08	0.28	-0.06	0.32	-0.04	0.29	-0.04
	GPS data	0.19	-0.06	0.14	-0.04	-	-	0.16	-0.05
2010/10/21 to 2011/03/24	TSX	3.76	-1.15	3.35	-0.79	3.22	-0.59	3.11	-0.49
	GPS data	3.42	-1.12	2.91	-0.77	-	-	2.61	-0.46

The detected motion points to the east as the location goes to the south. This trend matched with the observed GPS data. The standard deviation of the angular movement heading in each subarea was around 5°, showing that the displacement vectors pointed to almost the same direction. Many small differences in direction were caused by geocoding and resampling. However, several arrows still pointed to different directions, which were errors caused by the terrain.

Crustal movements were also detected in the periods October 21, 2010–March 24, 2011, and October 21, 2010–April 4, 2011. These three displacement vectors are shown in Fig. 5(a), while the displacement amplitude for the period October 21, 2010–April 4, 2011, is shown in Fig. 5(b). According to the GPS data, the crustal movement got larger with time passing by after the mainshock, which is consistent with the detected results from the SAR data for the three time periods.

To verify the applicability of our method to smaller displacement cases, the displacements between March 13, 2011, and March 24, 2011, were also calculated, and the results around the GPS stations are shown in Table I. The average shifts of 0.30 m to the east and 0.05 m to the south were obtained, showing only 0.12–0.14-m difference with the GPS data. This observation supports the applicability of the proposed method to grasp small surface displacements. The total displacements obtained in the periods October 21, 2010–March 13, 2011, and March 13–24, 2011, were close to those obtained in the period October 21, 2010–March 24, 2011.

V. VERIFICATION AND DISCUSSION

To verify the accuracy and usefulness of the proposed method, two TSX intensity images of central Tokyo and the crustal movement data from GPS stations were introduced.

A. Crustal Movements in Tokyo

The first TSX image of central Tokyo was captured on May 23, 2008 (UTC), while the second one was captured on November 23, 2009, with a 42.8° incident angle (Fig. 6). The images were taken in a descending path with HH polarization by strip-map mode and then transformed to EEC products by DLR. No major event such as an earthquake occurred during this period, so the shifts of buildings should be theoretically close to zero. We extracted 2041 buildings from the first image, and 1789 buildings were detected as unchanged. We then calculated the shifts of 1443 buildings which have the correlation coefficients larger than 0.8. The mean value of the

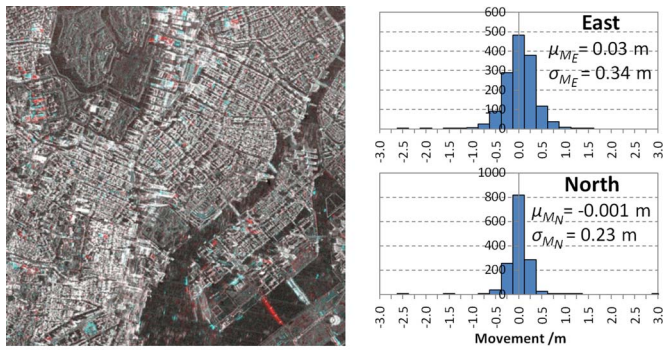

Fig. 6. (a) Color composite of TSX images covering central Tokyo taken on (green and blue) May 24, 2008, and (red) November 23, 2009. (b) Histograms of the displacement to the east and north directions.

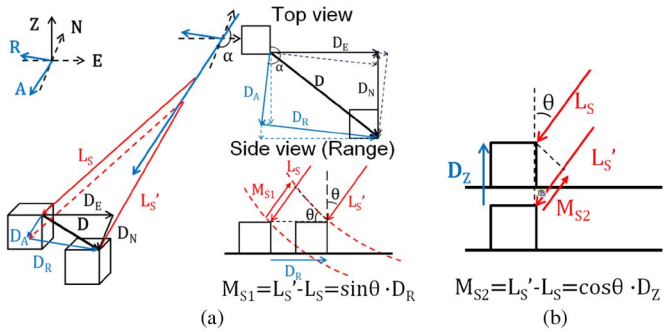

Fig. 7. Schematic views of the (a) horizontal and (b) vertical displacements in a SAR image.

displacement amplitude was 0.32 m (a possible location error), with an averaged shift of 0.03 m to the east and 0.001 m to the south. Only small shifts were observed for most buildings and were distributed evenly to all directions. This result further supports the fact that the displacements obtained by our method can be considered as crustal movements at a subpixel level accuracy.

B. Comparison With GPS Observation Data

Surface displacement is a vector in 3-D space with three components D_E, D_N, and D_Z to the east, north, and vertical directions, respectively. The relationship between an actual crustal movement and its shift in a SAR image is shown in Fig. 7. SAR intensity images are geocoded with a spacing to the north and east directions, so the relationship between a crustal movement (D) and its shift (M) in a ground-range SAR image can be described by

$$\begin{pmatrix} M_E \\ M_N \end{pmatrix} = \begin{pmatrix} 1 & 0 & \frac{\cos\alpha}{\tan\theta} \\ 0 & 1 & \frac{\sin\alpha}{\tan\theta} \end{pmatrix} \begin{pmatrix} D_E \\ D_N \\ D_Z \end{pmatrix} \quad (1)$$

where D is the actual movement to the east, north, and vertical directions; M is the shift in the SAR image; α is the heading angle clockwise from the north; and θ is the SAR incident angle.

The GPS recordings obtained at Yamoto, Rifu, Natori, and Watari stations from March 1 to April 25, 2011, were converted using (1) with a heading angle of 190.027° and a 37.313° incident angle, as shown in Fig. 8. There, stations other than Rifu stopped after the earthquake due to power outage and/or

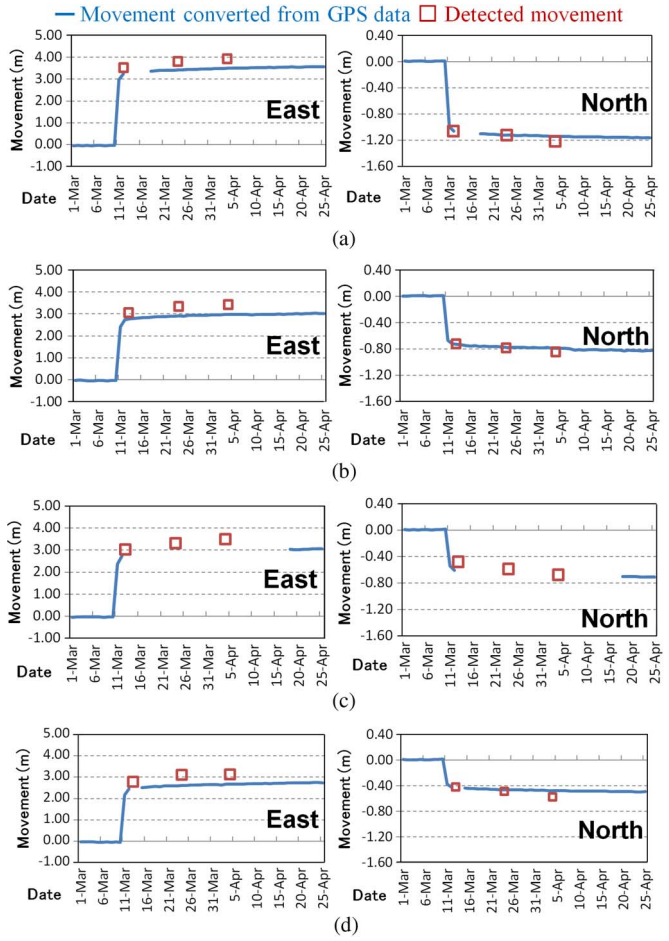

Fig. 8. Comparison of movements converted from GPS data at (a) Yamoto, (b) Rifu, (c) Natori, and (d) Watari ground control stations and the results detected in surrounding 25-km^2 subareas.

strong shaking. Natori GPS station was hit by tsunami and damaged, and thus, it did not restart until April 18, 2011. The measurement of crustal movements from SAR images provides an important and effective tool in such cases. A comparison of the results detected around the GPS stations with the converted GPS recordings demonstrated a very high level of consistency. Based on the ten comparison points in Fig. 8, the averaged differences between the detected result and the GPS measurement were about 0.38 m to the east and 0.02 m to the north. The maximum differences were 0.50 m to the east (Watari station) and 0.12 m to the north (Natori station), shown in Table I.

VI. Conclusion

In this letter, we have proposed a method for detecting crustal movements due to a major earthquake on the basis of a comparison between two temporal SAR intensity images. The method was tested using four temporal TSX images covering the coast of Miyagi Prefecture before and after the 2011 Tohoku earthquake, which is a very difficult case as the displacement exceeded the image area and two temporal images of Tokyo. Although it is impossible to detect the actual 3-D movement only from the descending pair, the four subareas surrounding GPS stations exhibited stable shifts of unchanged buildings and similar to the converted observed GPS data. Subpixel-based matching made it possible to detect movements with high accuracy, within 0.5 m. However, the accuracy of our method depends on the location accuracy of the original SAR images. Although the results obtained in this study are promising, we will further test the proposed method for other events including smaller surface displacements to validate its applicability. Also, a further study will be carried out to enhance the proposed method to 3-D cases.

Acknowledgment

The authors would like to thank Dr. M. Huber and Dr. H. Taubenböck of DLR for providing the location accuracy information of TerraSAR-X products.

References

[1] Geospatial Information Authority of Japan. [Online]. Available: http://www.gsi.go.jp/BOUSAI/h23_tohoku.html#namelink3
[2] H. A. Zebker, "Studying the Earth with interferometric radar," *IEEE Comput. Sci. Eng.*, vol. 2, no. 3, pp. 52–60, May/Jun. 2000.
[3] S. Stramondo, F. R. Cinti, M. Dragoni, S. Salvi, and S. Santini, "The August 17, 1999 Izmit, Turkey, earthquake: Slip distribution from dislocation modeling of DInSAR and surface offset," *Ann. Geophys.*, vol. 45, no. 3/4, pp. 527–536, 2002.
[4] M. Chini, S. Atzori, E. Trasatti, C. Bignami, C. Kyriakopoulos, C. Tolomei, and S. Stramondo, "The May 12, 2008, (M_w 7.9) Sichuan earthquake (China): Multiframe ALOS-PALSAR DInSAR analysis of coseismic deformation," *IEEE Geosci. Remote Sens. Lett.*, vol. 7, no. 2, pp. 266–270, Apr. 2010.
[5] R. Bürgmann, P. A. Rosen, and E. J. Fielding, "Synthetic aperture radar interferometry to measure Earth's surface topography and its deformation," *Annu. Rev. Earth Planet Sci.*, vol. 28, pp. 169–209, 2000.
[6] R. Michel, J.-P. Avouac, and J. Taboury, "Measuring ground displacements from SAR amplitude image: Application to the Landers earthquake," *Geophys. Res. Lett.*, vol. 26, no. 27, pp. 875–878, Apr. 1999.
[7] M. Tobita, H. Suito, T. Imakiire, M. Kato, S. Fujiwara, and M. Murakami, "Outline of vertical displacement of the 2004 and 2005 Sumatra earthquakes revealed by satellite radar imagery," *Earth Planets Space*, vol. 58, no. 1, pp. e1–e4, 2006.
[8] R. E. Crippen, "Measurement of subresolution terrain displacements using SPOT panchromatic imagery," *Int. J. Remote Sens.*, vol. 15, no. 1, pp. 56–61, 1992.
[9] S. Leprince, S. Barbot, F. Ayoub, and J.-P. Avouac, "Automatic and precise orthorectification, coregistration, and subpixel correlation of satellite images, application to ground deformation measurements," *IEEE Trans. Geosci. Remote Sens.*, vol. 45, no. 6, pp. 1529–1558, Jun. 2007.
[10] P. J. González, M. Chini, S. Stramondo, and J. Fernández, "Coseismic horizontal offsets and fault-trace mapping using phase correlation of IRS satellite images: The 1999 Izmit (Turkey) earthquake," *IEEE Trans. Geosci. Remote Sens.*, vol. 48, no. 5, pp. 2242–2250, May 2010.
[11] Y. Fialko, M. Simons, and D. Agnew, "The complete (3-D) surface displacement field in the epicentral area of the 1999 M_w 7.1 Hector Mine earthquake, California, from space geodetic observations," *Geophys. Res. Lett.*, vol. 28, no. 16, pp. 3063–3066, 2001.
[12] J. Catalão, G. Nico, R. Hanssen, and C. Catita, "Merging GPS and atmospherically corrected InSAR data to map 3-D terrain displacement velocity," *IEEE Trans. Geosci. Remote Sens.*, vol. 49, no. 6, pp. 2354–2360, Jun. 2011.
[13] M. de Michele, D. Raucoules, J. de Sigoyer, and M. Pubellier, "Three dimensional surface displacement of the 2008 May 12 Sichuan earthquake (China) derived from synthetic aperture radar: Evidence for rupture on a blind thrust," *Geophys. J. Int.*, vol. 183, no. 3, pp. 1097–1103, Dec. 2010.
[14] M. Eineder, T. Fritz, J. Mittermayer, A. Roth, E. Borner, H. Breit, and B. Brautigam, "TerraSAR-X ground segment basic product specification document," TX-GS-DD-3302, pp. 31–32, 2010, Issue 1.7.
[15] H. Breit, T. Fritz, U. Balss, M. Lachaise, A. Niedermeier, and M. Vonavka, "TerraSAR-X SAR processing and products," *IEEE Trans. Geosci. Remote Sens.*, vol. 48, no. 2, pp. 727–739, Feb. 2010.
[16] M. Wermuth, A. Hauschild, O. Montenbruck, and A. Jäggi, "TerraSAR-X rapid and precise orbit determination," in *Proc. 21st Int. Symp. Space Flight Dyn.*, Toulouse, France, 2009.